

Intermolecular potential energy surface and second virial coefficients for the water–CO₂ dimer^{a)}

Richard J. Wheatley^{1,b)} and Allan H. Harvey^{2,c)}

¹*School of Chemistry, The University of Nottingham, Nottingham, NG7 2RD, United Kingdom*

²*Thermophysical Properties Division, National Institute of Standards and Technology, Boulder, Colorado 80305, USA*

(Received 13 December 2010; accepted 15 March 2011; published online 7 April 2011)

A five-dimensional potential energy surface is calculated for the interaction of water and CO₂, using second-order Møller–Plesset perturbation theory and coupled-cluster theory with single, double, and perturbative triple excitations. The correlation energy component of the potential energy surface is corrected for basis set incompleteness. In agreement with previous studies, the most negative interaction energy is calculated for a structure with C_{2v} symmetry, where the oxygen atom of water is close to the carbon atom of CO₂. Second virial coefficients for the water–CO₂ pair are calculated for a range of temperatures, and their uncertainties are estimated. The virial coefficients are shown to be in close agreement with the available experimental data. © 2011 American Institute of Physics. [doi:10.1063/1.3574345]

I. INTRODUCTION

The noncovalent interaction between water and CO₂ molecules is of great scientific and commercial importance. Dissolved CO₂ is the main ingredient in photosynthesis, and is an important factor in determining the pH and corrosiveness of terrestrial water. The effervescence of CO₂ solutions is responsible for over 10¹¹ liters of carbonated drinks being consumed worldwide every year. Thermodynamic properties of gaseous mixtures containing water and CO₂ are important for the design of advanced power cycles that facilitate CO₂ sequestration, such as the oxy-fuel and integrated gasification combined cycle (IGCC) processes. In these systems, mixtures with water and CO₂ appear in the precombustion synthesis gas (in IGCC), in the combustion gas that drives the turbines, and in the postcombustion separation and compression of CO₂ for sequestration.^{1–3} In the condensed phase, since carbon dioxide in solution is almost entirely in the form of molecular CO₂, rather than carbonic acid or its conjugate bases, detailed and accurate information on the intermolecular forces between water and CO₂ is a crucial part of modeling the thermodynamic and phase coexistence properties of mixtures involving these two components.

The water–CO₂ dimer was observed using infrared spectroscopy in a solid oxygen matrix by Tso and Lee,⁴ and in the gas phase, in the radiofrequency and microwave region of the spectrum, by Peterson and Klemperer.⁵ These observations suggested that the dimer adopts a symmetrical, non-hydrogen-bonded structure in both environments. This has been confirmed by more recent studies,^{6,7} which investigated the internal motion of the molecules in the complex in more detail. Although these spectroscopic methods provide precise data on the lowest-energy geometries of the complex, they do

not sample the whole of the potential in detail, as is required for thermodynamic calculations.

Previous computational studies of the interaction between water and CO₂ molecules have also mainly concentrated on the region(s) where the interaction energy is most negative, not the complete five-dimensional potential energy surface. There has also been some disagreement over the existence of other equilibrium structures of the water–CO₂ dimer. In one early study, Makarewicz *et al.*⁸ found a nonplanar equilibrium structure in which the oxygen atom of water is close to the carbon atom of CO₂ (approximately “T-shaped”), but they did not find a hydrogen-bonded structure. Their calculations used second-order Møller–Plesset perturbation theory (MP2) with a fairly small basis set, and did not include a correction for the basis set superposition error (BSSE). As a result, their calculated binding energy of the dimer is probably 10%–20% too large. Sadlej and Mazurek⁹ also used MP2 calculations, with a larger basis set, and corrected the results for the BSSE. They found a symmetrical, T-shaped, planar minimum-energy structure, and a hydrogen-bonded local minimum. Kieninger and Ventura¹⁰ studied the equilibrium structure of the complex and some one-dimensional cuts through the potential energy surface using MP2, quadratic configuration interaction with single, double, and perturbative triple excitations, and density functional theory calculations. Their calculated dimer structure was also close to T-shaped but had no symmetry. In a more detailed theoretical study of the dimer, Sadlej *et al.*¹¹ used calculations up to the fourth-order perturbation theory to investigate several one-dimensional and two-dimensional cuts through the potential energy surface. They found both T-shaped and hydrogen-bonded equilibrium structures. Duan and Zhang¹² investigated the equation of state of water–CO₂ mixtures with an intermolecular potential energy function fitted to the calculations of Sadlej *et al.*,¹¹ although they used a simple Lennard-Jones plus point charge fitting function which cannot be expected to represent the potential energy surface accurately,

^{a)}Partial contribution of the National Institute of Standards and Technology, not subject to copyright in the United States.

^{b)}Electronic mail: Richard.Wheatley@nottingham.ac.uk.

^{c)}Electronic mail: aharvey@boulder.nist.gov.

and the calculated points that they used for fitting only cover a small amount of the surface. Recently, Schriver *et al.*¹³ performed MP2 calculations on T-shaped and unsymmetrical (near T-shaped) planar dimer structures, to support their infrared studies of the water–CO₂ dimer in a nitrogen matrix. They concluded that the two structures are very close in energy, with the unsymmetrical planar structure found to be slightly more stable, although they remarked that the minimum-energy geometry of the dimer depended on the method of calculation. They also performed coupled-cluster calculations with single, double, and perturbative triple excitations [CCSD(T)], which gave a considerably smaller interaction energy than the previous studies. This small binding energy may be an artefact of a small basis set. Altmann and Ford¹⁴ considered several dimer structures at the MP2 level, and also concluded that the equilibrium structure is planar and close to T-shaped.

While this work was in preparation, a five-dimensional potential energy surface was calculated by Makarewicz.¹⁵ The interaction energy was calculated at the MP2 level, and extrapolated to the complete basis set limit. The potential energy surface was then modified in an attempt to take account of additional correlation effects present in CCSD(T), by performing CCSD(T) calculations for several cuts through the potential energy surface. The low-energy region of the potential energy surface was explored, including details of minima and saddle points. This potential of Makarewicz is compared with our results later in this paper.

The aims of the current work are: first, to give a complete picture of the interaction of water and CO₂ by performing calculations covering the complete five-dimensional potential energy surface; second, to assess the remaining uncertainties in the calculated interaction energies by considering the effect of changing the basis set, the method used to calculate electron correlation, and the monomer geometries; third, to provide a fitted potential energy function which reproduces the calculated data closely; and finally, to calculate second virial coefficients for the water–CO₂ mixture, with the estimated uncertainties in the calculations taken into account, and compare them with the available experimental data.

II. THE POTENTIAL ENERGY SURFACE

Binding energies of the water–CO₂ dimer are calculated using MP2 and CCSD(T) methods. The aug-cc-pVTZ and aug-cc-pVQZ basis sets¹⁶ are both employed for the MP2 calculations, but computational limitations restrict the CCSD(T) calculations to the aug-cc-pVTZ basis set only. These basis sets are referred to below as TZ and QZ for brevity. Electron correlation contributions to the binding energy are calculated, and the full counterpoise correction for the basis set superposition error is employed in all cases. The MOLPRO program^{17,18} is used for the calculations.

Most of the calculations use fixed, vibrationally averaged, ground-state geometries for the two monomers, with an OH bond length of 1.8361 a_0 , a HOH bond angle of 104.69°,¹⁹ a CO bond length of 2.2114 a_0 ,²⁰ and an OCO bond angle of 180°, where a_0 is the Bohr radius, a_0

≈ 0.052917721 nm. The validity of using this monomer geometry for water has been checked for second virial coefficients of the water–CO mixture.²¹

The intermolecular dimer geometries are split into two sets. In Set 1, the length of a vector from the carbon atom of CO₂ to the oxygen atom of water has values from 4 a_0 to 10 a_0 in steps of 1 a_0 , and in Set 2, the length of a vector from an oxygen atom of CO₂ to the oxygen atom of water has the same seven values. The angle X between this vector and the CO₂ axis is restricted to values of $\cos(X) = 0$ and 0.25 in Set 1, and $\cos(X) = [0, 0.25, 0.5, 0.75, 1]$ in Set 2. The water molecule is initially placed with its symmetry axis parallel to the CO₂ molecular axis, such that the dimer is planar; then it is rotated into 180 different orientations defined by the Euler angles $\alpha = [0, \pi/4, \pi/2, 3\pi/4, \pi]$, $\cos(\beta) = [0, \pm 1/4, \pm 1/2, \pm 3/4, \pm 1]$, $\gamma = [0, \pi/4, \pi/2, 3\pi/4]$. The Euler angles are defined with respect to a z-axis parallel to the water symmetry axis and an x-axis in the plane of the water molecule. This gives 8820 intermolecular geometries, 5285 of which are symmetry-distinct.

The accuracy of the calculated interaction energies is affected by the size of the basis set, so an attempt is made to correct the calculated energies for the basis set incompleteness and to estimate the complete basis set (CBS) limit of the interaction energy. The size of the basis set has more effect on the electron correlation contribution E_{corr} to the interaction energy than it does on the self-consistent field (SCF) contribution E_{SCF} . For example, in a T-shaped dimer geometry, with a near-equilibrium intermolecular C–O separation of 5.26 a_0 , the difference between the MP2/TZ and MP2/QZ interaction energies is about 170 μE_h , whereas the difference between the SCF/TZ and SCF/QZ interaction energies is only 17 μE_h . (The Hartree energy, E_h , is approximately 4.359748×10^{-18} J.) The SCF/QZ interaction energy is used, without modification, as an approximation to the SCF/CBS interaction energy (a few additional calculations at the SCF/5Z level suggest that this is a good approximation, with an error of about 12 μE_h near the minimum). The basis set error in E_{corr} is then assumed to be proportional to $1/C^3$,²² where C , the cardinality of the basis set, is 3 for TZ and 4 for QZ. The MP2/CBS interaction energy is therefore estimated from

$$E_{\text{MP2/CBS}} = E_{\text{MP2/QZ}} + \frac{27}{64 - 27} (E_{\text{MP2/QZ}} - E_{\text{MP2/TZ}}). \quad (1)$$

The MP2 and CCSD(T) methods give significantly different interaction energies, with the CCSD(T) energy expected to be closer to the “exact” full configuration interaction limit. For example, at the same T-shaped geometry as described above, the CCSD(T)/TZ interaction energy is roughly 255 μE_h more negative than the MP2/TZ interaction energy. However, an equation analogous to Eq. (1) cannot be used to estimate the CCSD(T)/CBS interaction energy, since CCSD(T)/QZ results are not available. The CCSD(T)/CBS interaction energy is estimated by assuming that the difference between MP2 and CCSD(T) interaction energies is

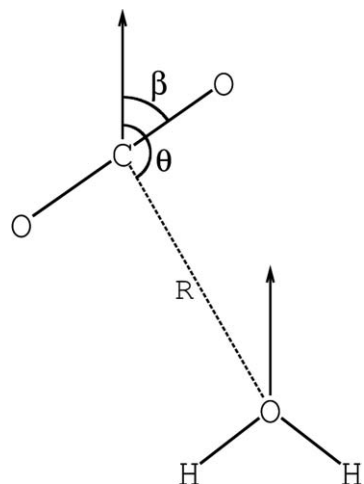


FIG. 1. Coordinate system used to describe planar water-CO₂ geometries. The arrows are parallel to the water symmetry axis.

independent of the basis set:

$$E_{\text{CCSD(T)/CBS}} = E_{\text{CCSD(T)/TZ}} + E_{\text{MP2/CBS}} - E_{\text{MP2/TZ}}. \quad (2)$$

In order to assess this approximation, 13 CCSD(T)/QZ calculations are performed at planar dimer geometries given by $120^\circ \leq \theta \leq 180^\circ$, with R and β chosen to be near the calculated minimum of the interaction energy for each θ value. The coordinates are defined in Fig. 1. The error in Eq. (2) (with the QZ basis used instead of the CBS limit) is less than $21 \mu E_h$ in all cases, and repeating the calculations for a few different separations R shows that the error decreases slowly as R increases.

At the above T-shaped geometry, the total CCSD(T)/CBS interaction energy is calculated to be approximately $-4540 \mu E_h$, with a SCF contribution of $-2810 \mu E_h$. The SCF/TZ, SCF/QZ, MP2/TZ, MP2/QZ, CCSD(T)/TZ, and estimated CCSD(T)/CBS results are available as supplementary data.²³

A possible source of error in the calculations is the assumption that the interacting molecules are rigid. In order to assess the size of this error, a series of MP2/QZ calculations is performed at different monomer geometries, near the T-shaped geometry. This dimer geometry is chosen because it is close to the minimum of the potential energy surface, so it contributes a relatively large amount to the second virial coefficient. The distortion of the monomer geometries is also expected to be relatively significant in the T-shaped geometry, because the intermolecular forces can readily deform the CO₂ molecule along its “soft” bending coordinate. Allowing the monomers to be flexible causes the CO₂ molecule to bend by about 2° , with the oxygen atoms of CO₂ moving further away from the water molecule. This distortion is similar to, but slightly smaller than, that calculated by Sadlej *et al.*²⁴ The total energy (calculated as the sum of the counterpoise-corrected interaction energy and the two monomer energies calculated in the monomer basis sets) is reduced by approximately $75 \mu E_h$ as a result of this monomer distortion.

Bearing in mind the above approximations in the calculation, an estimate of the uncertainty in the interaction energy

is taken to be 10% of E_{corr} ; the uncertainty near the potential minimum is therefore estimated to be $170 \mu E_h$.

The CCSD(T)/CBS interaction energy between the two rigid monomers is fitted to a function involving products of inverse powers of internuclear distances r_{ab} :

$$E_{\text{fit,CCSD(T)/CBS}} = \sum_{n,a,b} C_{n,ab} r_{ab}^{-n} + \sum_{n,n',a,a',b,b'} C_{nn',aa'bb'} r_{ab}^{-n} r_{a'b'}^{-n'}, \quad (3)$$

where a and a' are nuclei of CO₂ and b and b' are nuclei of water. In the first sum, n takes the values 1, 6, and 12. In the second sum, n and n' take the values (1,5), (2,4), (3,3), (4,4), (4,8), and (6,6). This functional form is chosen in preference to an anisotropic atom-atom function because it is found to give a better fit using fewer parameters, although calculations of the second virial coefficients (see below) are reasonably independent of the fitting method, within the estimated uncertainties. The calculated energies are fitted by minimizing the root-mean-square deviation between calculated and fitted values, with a relative weight of $1/(0.01 + E/E_h)^2$ assigned to each calculated interaction energy E , to improve the fit of the more important points near the bottom of the potential well relative to the repulsive wall. The values of n and n' in the second sum are chosen from several different possibilities involving overall inverse powers of 6, 8, 10, and 12, using trial and error. Again, the different choices of n and n' produce relatively small differences in the virial coefficients. The $C_{1,ab}$ coefficients in the first sum represent charge-charge interactions and are constrained to give charge neutrality for both molecules, so there is only one free-fitted $C_{1,ab}$ parameter ($C_{1,ab} = -0.41 E_h a_0$ when a is C and b is O). The sum of the $C_{6,ab}$ coefficients in the first sum and the $C_{15,aa'bb'}$, $C_{24,aa'bb'}$, and $C_{33,aa'bb'}$ coefficients in the second sum is the isotropic molecule-molecule long-range C_6 coefficient, which is a sum of induction and dispersion contributions. It is fixed at $-92 E_h a_0^6$, which is estimated from the water dipole moment and from calculated static and frequency-dependent polarizabilities of the two monomers. The value of C_6 can be varied considerably (by at least $\pm 50\%$) with negligible effect on the virial coefficients. The final root-mean-square error in fitting these 110 symmetry-distinct C parameters to the calculated interaction energies is $111 \mu E_h$. A FORTRAN program to evaluate the fitted potential, and the fitted parameters, is published as supplementary data.²³

The fitted intermolecular potential is about $-4456 \mu E_h$ for a C_{2v} dimer geometry with $R \approx 5.26 a_0$, $\theta = 180^\circ$, and $\beta = 90^\circ$: see Fig. 1. The calculated CCSD(T)/CBS intermolecular potential at this geometry is $-4522 \mu E_h$. However, this is not the global minimum of the fitted potential. The fitting procedure gives a planar minimum with $E \approx -4508 \mu E_h$, $R \approx 5.29 a_0$, $\theta \approx 150^\circ$, and $\beta = 55^\circ$. The calculated interaction energy at this geometry is $-4454 \mu E_h$, which is above the energy of the C_{2v} geometry, and it appears that the lower-symmetry minimum is a fitting artefact. The potential energy surface in this region is quite flat, as pointed out by Makarewicz *et al.*⁸

The barrier to interconversion of the two equivalent C_{2v} minima, which is reached by rotating the water molecule by 90° about its symmetry axis, agrees within 3% with the previous calculations by Sadlej *et al.*¹¹ The fitted potential energy surface gives a barrier of $1455 \mu E_h$ if R is fixed during the rotation, and $1263 \mu E_h$ if R is optimized at the saddle point.

In recent work,¹⁵ Makarewicz calculated a five-dimensional potential energy surface at the MP2 level and applied a correction to estimate the CCSD(T) potential at the complete basis set limit. The resulting potential energy surface was investigated to give details of the potential energy minimum, cuts through the surface describing radial and angular motions of the two molecules, and the potential energy barriers and bifurcations of minimum energy paths associated with some of these motions. Our MP2 results agree well with the MP2 calculations of Makarewicz, even though the monomer geometries and basis sets are different. However, there is a significant difference between the fitted CCSD(T) potential energy surfaces at long range. From orientational averaging of long-range energy calculations ($R > 20 a_0$), the C_6 coefficient in the Makarewicz potential appears to be $-2000 E_h a_0^6$ or larger, which is at least 20 times the correct value.

At smaller separations, the potential energy surfaces are in relatively better agreement. Makarewicz showed (Fig. 4 of Ref. 15) that, as the molecules are pulled apart, the minimum energy path bifurcates at a C–O distance of about $5.8 a_0$. This bifurcation occurs at about $4.6 a_0$ in our fitted potential, although, as stated above, the difference is mainly an artefact of our fit. Apart from this difference in the bifurcation point, the change in the bending angle is qualitatively the same for the two potentials as a function of separation. The two potentials agree well along the CO₂ rotation and the water wagging and tilting coordinates shown in Figs. 6, 7, and 8 of Ref. 15. The combination of water tilt angle and out-of-plane torsion was also considered by Makarewicz. A bifurcation of the saddle point was found, corresponding to the abovementioned barrier to the interconversion of equivalent minima. The symmetrical saddle point was predicted to be a second-order saddle point, linking two first-order saddle points. Our fitted potential energy surface does not predict this bifurcation, but the potential energy surface in this region is very flat, and the calculations agree to well within our estimated uncertainty. It should be emphasized that the main aim of our fitting procedure is to provide a global description of the potential energy surface of sufficient accuracy to calculate second virial coefficients, not to locate stationary points.

III. SECOND VIRIAL COEFFICIENTS

A. Calculation

The cross second virial coefficient $B_{12}(T)$ for the water–CO₂ mixture is calculated with the procedure described previously,²⁵ including translational and rotational quantum effects to first order, and also using an effective potential method, which is correct to first order, to estimate the higher-order quantum corrections.²⁶ There is little difference between the two results; the effective potential calculations are reported here.

TABLE I. Coefficients for Eq. (4) for $B_{12}(T)$ for the water–CO₂ pair. The c_i are in $\text{cm}^3 \text{mol}^{-1}$ and the d_i are dimensionless.

i	c_i	d_i
1	47.54	−0.126
2	−658.04	−1.34
3	−3969.1	−3.75
4	−24225.	−7.6

The fitted intermolecular potential behaves unphysically, and can become strongly attractive, when the two molecules come very close together. In order to ensure that this does not affect the calculations of the second virial coefficients, whenever the repulsive wall of the fitted potential reaches a maximum, the intermolecular potential is set to infinity for all shorter intermolecular separations. The lowest-energy unphysical maximum is found in the fit at approximately $13000 \mu E_h$, and the error produced in the virial coefficients by replacing such a large energy by an infinite value is negligible at the temperatures considered.

The B_{12} values are fitted as a function of temperature:

$$B_{12}(T) = \sum_{i=1}^4 c_i (T^*)^{d_i}, \quad (4)$$

where $T^* = T/(100 \text{ K})$, B_{12} and the c_i have units of $\text{cm}^3 \text{mol}^{-1}$, and the values of c_i and d_i are given in Table I. Equation (4) reproduces the calculated values within a tolerance that is much smaller than their uncertainty. It is valid from 200 to 2000 K, and extrapolates in a physically reasonable manner beyond that range. Table II shows calculated values of $B_{12}(T)$, along with their expanded uncertainties. Expanded uncertainties in the second virial coefficients are estimated, for reasons discussed above, using two modified intermolecular potentials: one (everywhere deeper) potential with the correlation energy contribution to the intermolecular potential increased by 10%, and a second (everywhere shallower) potential where the correlation contribution is decreased by 10%. The modified potentials are used to calculate estimated lower and upper bounds on the second virial coefficients by first fitting them to the same function as described above; the accuracy of all the fits is essentially the same. The resulting bounds on the second virial coefficients are conservatively assumed to represent an expanded uncertainty with coverage factor $k = 2$, approximately equal to a 95% confidence interval.

B. Comparison with experimental data

Data for B_{12} for water–CO₂ can be derived from vapor-phase composition measurements of liquid water in equilibrium with gaseous CO₂. We apply the procedure described previously²⁷ to several sources of such data;^{28–31} the resulting values of B_{12} are shown in Table III along with our estimates of their uncertainty (standard uncertainty with coverage factor 2, reflecting only uncertainty in the measurement of water content but not additional factors, such as neglect of higher virial coefficients).

TABLE II. Second virial coefficients B_{12} calculated with Eq. (4) and their expanded uncertainties $U(B_{12})$.

T (K)	B_{12} ($\text{cm}^3 \text{mol}^{-1}$)	$U(B_{12})$ ($\text{cm}^3 \text{mol}^{-1}$)
200	−636.2	137.0
250	−301.1	55.6
300	−179.8	31.9
350	−120.2	21.8
400	−85.3	16.5
450	−62.7	13.3
500	−46.9	11.2
600	−26.5	8.6
700	−14.0	7.0
800	−5.6	6.0
900	0.4	5.2
1000	4.8	4.7
1500	16.2	3.1
2000	20.7	2.4

In addition, we compare to B_{12} derived by Vanderzee and Haas³² from volumetric data in the literature^{33–36} and to B_{12} reported by Patel *et al.*³⁷ from their isochoric expansion measurements. Patel *et al.*³⁷ reported B_{12} from two different methods of analysis; we average the two values at each temperature for use in this work.

Koglbauer and Wendland³⁸ reported spectroscopically measured concentration enhancement factors (the ratio of equilibrium water concentration in CO_2 to that above pure water) at six temperatures from 25 to 100 °C. Most of the data are at pressures sufficiently low (below 5 MPa) so that the nonideality should primarily reflect effects at the second virial level. In order to convert these data to mole fractions as needed for extracting B_{12} , the molar density of the vapor

TABLE III. Water– CO_2 second virial coefficients derived from the experimental phase-equilibrium data.

T (K)	B_{12} ($\text{cm}^3 \text{mol}^{-1}$)	Uncertainty in B_{12} ($\text{cm}^3 \text{mol}^{-1}$)	Reference
288.70	−265.1	7.1	29
298.14	−232.3	7.3	29
298.14	−240.9	6.9	28
298.28	−178.1	36.0	31
302.59	−224.1	6.9	29
304.20	−203.2	6.7	29
308.21	−154.8	14.6	31
318.22	−203.7	14.1	31
323.14	−160.0	6.7	28
323.2	−162.3	30.9	30
333.2	−134.7	21.6	30
348.13	−120.9	6.3	28
348.13	−136.6	7.7	29
353.1	−110.0	13.6	30
366.46	−94.7	8.3	29
373.12	−96.4	5.8	28
394.23	−99.8	9.5	29
422.01	−78.9	11.6	29
477.55	−52.3	27.7	29

phase is required; this can be estimated from the virial expansion with the unknown water mole fraction solved self-consistently with the composition-dependent mixture second virial coefficient. However, the resulting B_{12} varies strongly with pressure and is generally more negative than other data. This pressure dependence does not appear in other data sets and is too large to be accounted for by third virial effects (which are known at the high end of the temperature range in question³⁷). We conclude that a problem exists either with the experiments or with our procedure for converting the concentration enhancement factors to B_{12} . Therefore, we cannot compare our B_{12} with these experiments.

The B_{12} values reported by Skripka³⁹ and by Zawisza and Malesińska⁴⁰ are not included here because they seem to be outliers; the values in Ref. 39 also have an unphysically strong temperature dependence. The dew-point data of Jarne *et al.*⁴¹ are not used because they were taken at conditions where the equilibrium condensed phase would be a gas hydrate.

Vapor-phase enthalpy-of-mixing data, when extrapolated to low pressure, yield the quantity $\phi_{12} = B_{12} - T(dB_{12}/dT)$. At temperatures from approximately 363–393 K, we use ϕ_{12} and its uncertainty as reported by Wormald and Lancaster,⁴² who reanalyzed the measurements of Smith and Wormald.⁴³ At higher temperatures and pressures, excess enthalpies for this mixture were reported by Lancaster and Wormald⁴⁴ and by Wilson and Brady.⁴⁵ As described previously,²⁷ we extrapolate these data to zero pressure in order to extract ϕ_{12} . Table IV lists the values of ϕ_{12} , along with their uncertainties which result primarily from uncertainty in the zero-pressure extrapolation.

For all calculations, $B(T)$ and dB/dT for pure water are calculated from the correlation of Harvey and Lemmon.⁴⁶ Properties of pure CO_2 , including $B(T)$, are calculated from the reference-quality equation of state of Span and Wagner.⁴⁷ For phase-equilibrium studies where the liquid composition was not measured,^{28,38} the Henry's-constant correlation of

TABLE IV. Values of $\phi_{12} = B_{12} - T(dB_{12}/dT)$ for water– CO_2 derived from the vapor-phase enthalpy-of-mixing data.

T (K)	ϕ_{12} ($\text{cm}^3 \text{mol}^{-1}$)	Uncertainty in ϕ_{12} ($\text{cm}^3 \text{mol}^{-1}$)	Reference
363.4	−317	66	42
375.2	−287	31	42
383.2	−270	30	42
392.6	−262	39	42
448.16	−240	32	44
473.16	−195	22	44
498.16	−175	18	44
523.16	−139	15	44
548.16	−123	19	44
573.16	−123	15	44
598.16	−116	15	44
648.16	−92	11	44
693.2	−90	15	45
698.15	−87	11	44
804.1	−49	12	45
914.0	−27	15	45

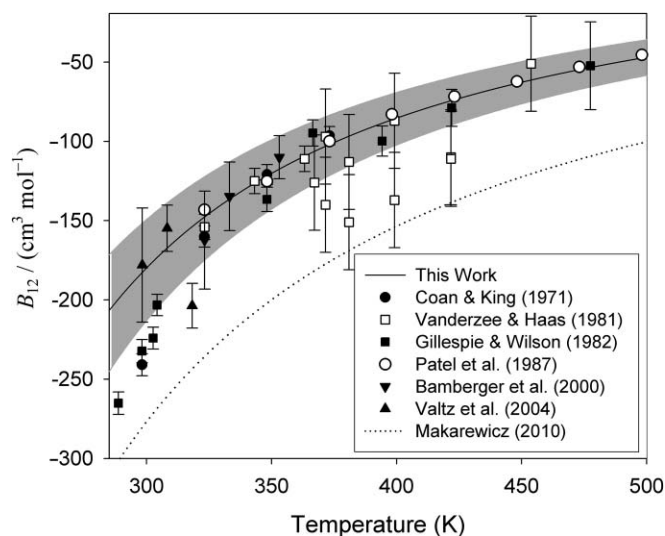


FIG. 2. Comparison of values of B_{12} calculated in this work with values derived from the Makarewicz potential and from the experimental data at low and moderate temperatures. The shading represents the expanded ($k = 2$) uncertainty in the calculated results.

Fernández-Prini *et al.*⁴⁸ is used to estimate the aqueous solubility of CO_2 .

Figures 2 and 3 show our calculated values of B_{12} along with the available experimental data. The shaded area represents the uncertainty in our results, based on calculations with the electron correlation part of the interaction energy perturbed to be more positive and more negative by 10% as explained above. Both our uncertainties and those of the literature points may be taken as expanded uncertainties with coverage factor $k = 2$ (approximately a 95% confidence interval). Agreement with the available data is good; we agree especially well with the careful expansion experiments of Patel *et al.*,³⁷ for which no error bars are drawn because none were reported in the paper (only a standard deviation of a re-

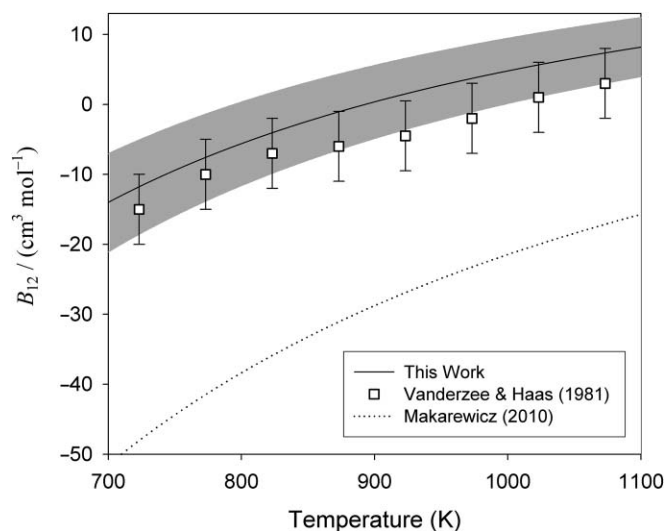


FIG. 3. Comparison of values of B_{12} calculated in this work with values derived from the Makarewicz potential and from the available high-temperature experimental data. The shading represents the expanded ($k = 2$) uncertainty in the calculated results.

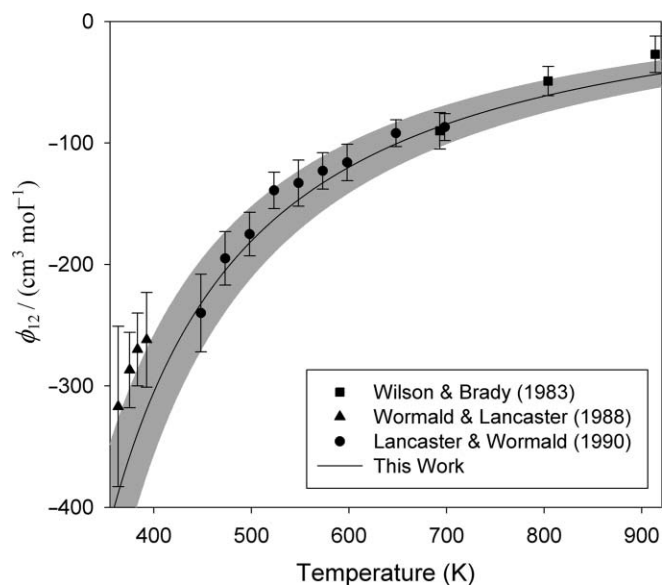


FIG. 4. Comparison of values of ϕ_{12} calculated in this work with values derived from the experimental data. The shading represents the expanded ($k = 2$) uncertainty in the calculated results.

gression was reported). At the lowest temperatures, we disagree modestly with the limited data available,^{28,29} we note that one of these sources²⁹ is from the same laboratory where we have observed similar deviations in low-temperature values of B_{12} for water with H_2 (Ref. 25) and with CO .²¹

Figure 4 shows a similar comparison for ϕ_{12} . Agreement with the available experimental data for this quantity^{42,44,45} is excellent.

Second virial coefficients calculated from the potential of Makarewicz¹⁵ are also shown in Figs. 2 and 3. These are much lower than our estimated lower bounds, and are also lower than the experimental data. The discrepancy arises mainly from the long-range part of the Makarewicz potential, which was discussed at the end of Sec. II. This means that, despite its accuracy in the vicinity of the energy minimum, the Makarewicz potential cannot be used for thermodynamic calculations, which average over all intermolecular geometries including large separations.

IV. CONCLUSIONS

The equilibrium structure of the water- CO_2 dimer calculated in this work agrees closely with previous results in the literature, being planar and symmetrically “T-shaped” with an intermolecular O-C distance of about $5.3 a_0$. Although CO_2 is nonpolar and both molecules are reasonably small, the interaction between them is relatively strong. The potential well depth of about $-4500 \mu E_h$ is over 50% larger than the calculated well depth of the water-CO dimer,²¹ and is about half the strength of the water-water hydrogen bond. Furthermore, the dimer does not have the “(nearly)-hydrogen-bonded” structure that is found in other dimers of water, such as water-rare gas, water-oxygen, water-nitrogen, water-CO, and the water dimer itself. It is closer to the structure of the water- H_2 dimer,²⁵ although in water- H_2 , the hydrogen molecule is aligned along the symmetry axis of the

water molecule. These differences are probably caused by the strong electrostatic attraction between the oxygen atom of water and the carbon atom of CO₂, while the opposite signs for the quadrupoles of CO₂ and H₂ explain the different alignments these molecules adopt in their dimers with water. The extreme flatness of the water-CO₂ potential energy surface to the in-plane bending of the intermolecular bond has also been predicted before, and may, in part, be a result of the closer approach of a hydrogen atom of water and an oxygen atom of CO₂ when the dimer is bent.

In view of the relatively strong water-CO₂ interaction, it is necessary to investigate whether the thermodynamic properties of gas-phase water-CO₂ mixtures could be affected by any change in the geometries of the monomers, induced by their mutual attraction. To answer this question fully would require calculating a potential energy surface with many intramolecular degrees of freedom, and obtaining the rovibrational modes of the dimer from it. Accurate calculations on this scale are out of reach of current computational resources. Around the minimum-energy geometry, this work suggests that the uncertainties associated with monomer distortion may be of a similar size to those involved in the electronic-structure calculations that are used to obtain the rigid-molecule interaction energies. However, the effects of distortion will certainly be of less relative importance at larger molecular separations, which contribute a large amount to the virial coefficients, so overall, the resulting uncertainties may have been overestimated in this work. Further investigation of this effect would be useful.

Calculated second virial coefficients for the water-CO₂ dimer have larger estimated uncertainties than those for other water-containing dimers. This is partly a result of the monomer distortion problem just mentioned; the larger size of the CO₂ molecule also makes electronic-structure calculations more demanding, and the greater well depth of the intermolecular potential makes the second virial coefficients more sensitive to approximations made in calculating the energy, and in the fitting procedure. Nevertheless, the uncertainties in these calculations of $B_{12}(T)$ are smaller than the spread of the experimental data, and can be applied to a wide and continuous range of temperatures.

ACKNOWLEDGMENTS

The authors thank E. W. Lemmon for assistance in fitting Eq. (4). Partial financial support for this work was provided by the National Energy Technology Laboratory of the U.S. Department of Energy and by the Engineering and Physical Sciences Research Council.

- ¹J. Martinez-Frias, S. M. Aceves, J. R. Smith, and H. Brandt, *ASME J. Eng. Gas Turbines Power* **126**, 2 (2004).
²R. A. Dennis and R. Harp, in *Proceedings of the ASME Turbo Expo 2007, Montreal, Canada* (ASME, New York, 2007), Vol. 2, pp. 1093–1104.
³J. D. Figueroa, T. Fout, S. Plasynski, H. McIlvried, and R. D. Srivastava, *Int. J. Greenhouse Gas Control* **2**, 9 (2008).
⁴T.-L. Tso and E. K. C. Lee, *J. Phys. Chem.* **89**, 1612 (1985).

- ⁵K. I. Peterson and W. Klemperer, *J. Chem. Phys.* **80**, 2439 (1984).
⁶P. A. Block, M. D. Marshall, L. G. Pedersen, and R. E. Miller, *J. Chem. Phys.* **96**, 7321 (1992).
⁷G. Columberg, A. Bauder, N. Heineking, W. Stahl, and J. Makarewicz, *Mol. Phys.* **93**, 215 (1998).
⁸J. Makarewicz, T.-K. Ha, and A. Bauder, *J. Chem. Phys.* **99**, 3694 (1993).
⁹J. Sadlej and P. Mazurek, *J. Mol. Struct.: Theochem* **337**, 129 (1995).
¹⁰M. Kieninger and O. N. Ventura, *J. Mol. Struct.: Theochem* **390**, 157 (1997).
¹¹J. Sadlej, J. Makarewicz, and G. Chałasiński, *J. Chem. Phys.* **109**, 3919 (1998).
¹²Z. Duan and Z. Zhang, *Geochim. Cosmochim. Acta* **70**, 2311 (2006).
¹³A. Schriver, L. Schriver-Mazzuoli, P. Chaquin, and E. Dumont, *J. Phys. Chem. A* **110**, 51 (2006).
¹⁴J. A. Altmann and T. A. Ford, *J. Mol. Struct.: Theochem* **818**, 85 (2007).
¹⁵J. Makarewicz, *J. Chem. Phys.* **132**, 234305 (2010).
¹⁶T. H. Dunning, *J. Chem. Phys.* **90**, 1007 (1989).
¹⁷MOLPRO, a package of ab initio programs designed by H.-J. Werner and P. J. Knowles, version 2002.6, R. Lindh, M. Schütz, *et al.* See <http://www.molpro.net>.
¹⁸Certain commercial products are identified in this paper, but only in order to adequately specify the procedure. Such identification neither constitutes nor implies recommendation or endorsement by either the U.S. government or the National Institute of Standards and Technology.
¹⁹E. M. Mas and K. Szalewicz, *J. Chem. Phys.* **104**, 7606 (1996).
²⁰G. Herzberg, *Molecular Spectra and Molecular Structure II. Infrared and Raman Spectra of Polyatomic Molecules* (Van Nostrand, Princeton, NJ, 1945).
²¹R. J. Wheatley and A. H. Harvey, *J. Chem. Phys.* **131**, 154305 (2009).
²²A. Halkier, T. Helgaker, P. Jørgensen, W. Klopper, H. Koch, J. Olsen, and A. K. Wilson, *Chem. Phys. Lett.* **286**, 243 (1998).
²³See supplementary material at <http://dx.doi.org/10.1063/1.3574345> for the calculated interaction energies and a FORTRAN program to evaluate the fitted potential.
²⁴J. Sadlej, B. Rowland, J. P. Devlin, and V. Buch, *J. Chem. Phys.* **102**, 4804 (1995).
²⁵M. P. Hodges, R. J. Wheatley, G. K. Schenter, and A. H. Harvey, *J. Chem. Phys.* **120**, 710 (2004).
²⁶G. K. Schenter, *J. Chem. Phys.* **117**, 6573 (2002).
²⁷M. P. Hodges, R. J. Wheatley, and A. H. Harvey, *J. Chem. Phys.* **117**, 7169 (2002).
²⁸C. R. Coan and A. D. King, Jr., *J. Am. Chem. Soc.* **93**, 1857 (1971).
²⁹P. C. Gillespie and G. M. Wilson, Tech. Report RR-48, Gas Processors Association, Tulsa, OK (1982).
³⁰A. Bamberger, G. Sieder, and G. Maurer, *J. Supercrit. Fluids* **17**, 97 (2000).
³¹A. Valtz, A. Chapoy, C. Coquelet, P. Paricaud, and D. Richon, *Fluid Phase Equilib.* **226**, 333 (2004).
³²C. E. Vanderzee and N. C. Haas, *J. Chem. Thermodyn.* **13**, 203 (1981).
³³O. Maass and J. H. Mennie, *Proc. R. Soc. London* **110**, 198 (1926).
³⁴H. T. Gerry, Ph.D. Thesis, Massachusetts Institute of Technology (1932).
³⁵H. J. Greenwood, *Am. J. Sci.* **267A**, 191 (1969).
³⁶H. J. Greenwood, *Am. J. Sci.* **273**, 561 (1973).
³⁷M. R. Patel, J. C. Holste, K. R. Hall, and P. T. Eubank, *Fluid Phase Equilib.* **36**, 279 (1987).
³⁸G. Koglbauer and M. Wendland, *J. Chem. Eng. Data* **53**, 77 (2008).
³⁹V. G. Skripka, *Zh. Fiz. Khim.* **53**, 1407 (1979).
⁴⁰A. Zawisza and B. Malesińska, *J. Chem. Eng. Data* **26**, 388 (1981).
⁴¹C. Jarne, S. T. Blanco, M. Artal, E. Rauzy, S. Otín, and I. Velasco, *Fluid Phase Equilib.* **216**, 85 (2004).
⁴²C. J. Wormald and N. M. Lancaster, *J. Chem. Soc., Faraday Trans. 1* **84**, 3141 (1988).
⁴³G. R. Smith and C. J. Wormald, *J. Chem. Thermodyn.* **16**, 543 (1984).
⁴⁴N. M. Lancaster and C. J. Wormald, *J. Chem. Eng. Data* **35**, 11 (1990).
⁴⁵G. M. Wilson and C. J. Brady, Tech. Report RR-73, Gas Processors Association, Tulsa, OK (1983).
⁴⁶A. H. Harvey and E. W. Lemmon, *J. Phys. Chem. Ref. Data* **33**, 369 (2004).
⁴⁷R. Span and W. Wagner, *J. Phys. Chem. Ref. Data* **25**, 1509 (1996).
⁴⁸R. Fernández-Prini, J. L. Alvarez, and A. H. Harvey, *J. Phys. Chem. Ref. Data* **32**, 903 (2003).